THE JOURNAL OF BIOLOGICAL CHEMISTRY VOL. 286, NO. 34, pp. 30071–30086, August 26, 2011
© 2011 by The American Society for Biochemistry and Molecular Biology, Inc. Printed in the U.S.A.

# Myocyte Enhancer Factor 2C, an Osteoblast Transcription Factor Identified by Dimethyl Sulfoxide (DMSO)-enhanced Mineralization*

Received for publication, April 21, 2011, and in revised form, May 17, 2011 Published, JBC Papers in Press, June 7, 2011, DOI 10.1074/jbc.M111.253518

**Alexandre S. Stephens[‡], Sebastien R. Stephens[‡], Carl Hobbs[§], Deitmar W. Hutmacher[¶], Desa Bacic-Welsh[‡], Maria Ann Woodruff[¶], and Nigel A. Morrison[‡1]**

*From the [‡]School of Medical Science, Griffith University, Gold Coast Campus, Queensland 4215, Australia, [§]Guy's Campus, Kings College, WC2R 2LS London, United Kingdom, and the [¶]Institute for Health and Biomedical Innovation, Queensland University of Technology, Brisbane, Queensland 4001, Australia*

**Rapid mineralization of cultured osteoblasts could be a useful characteristic in stem cell-mediated therapies for fracture and other orthopedic problems. Dimethyl sulfoxide (DMSO) is a small amphipathic solvent molecule capable of stimulating cell differentiation. We report that, in primary human osteoblasts, DMSO dose-dependently enhanced the expression of osteoblast differentiation markers alkaline phosphatase activity and extracellular matrix mineralization. Furthermore, similar DMSO-mediated mineralization enhancement was observed in primary osteoblast-like cells differentiated from mouse mesenchymal cells derived from fat, a promising source of starter cells for cell-based therapy. Using a convenient mouse pre-osteoblast model cell line MC3T3-E1, we further investigated this phenomenon showing that numerous osteoblast-expressed genes were elevated in response to DMSO treatment and correlated with enhanced mineralization. Myocyte enhancer factor 2c (*Mef2c*) was identified as the transcription factor most induced by DMSO, among the numerous DMSO-induced genes, suggesting a role for *Mef2c* in osteoblast gene regulation. Immunohistochemistry confirmed expression of *Mef2c* in osteoblast-like cells in mouse mandible, cortical, and trabecular bone. shRNAi-mediated *Mef2c* gene silencing resulted in defective osteoblast differentiation, decreased alkaline phosphatase activity, and matrix mineralization and knockdown of osteoblast specific gene expression, including osteocalcin and bone sialoprotein. A flow on knockdown of bone-specific transcription factors, Runx2 and osterix by shRNAi knockdown of *Mef2c*, suggests that *Mef2c* lies upstream of these two important factors in the cascade of gene expression in osteoblasts.**

Skeletal patterning and subsequent cellular differentiation during development is a complex process involving the activation and suppression of gene regulatory programs leading to bone formation (1). Once fully developed, bone remains a dynamic tissue by undergoing continual remodeling, which functions to repair microarchitectural defects and maintain skeletal integrity (2). Numerous cell types are involved in the formation and homeostasis of the skeleton. Among these are osteoblasts (bone-forming cells), which differentiate from committed mesenchymal osteoprogenitor cells (1). The differentiation of osteoblasts is a highly coordinated process involving a clearly defined temporal sequence of events characterized by the commitment, proliferation, and subsequent maturation of precursor cells into terminally differentiated osteoblasts (3, 4). During this process, early differentiating cells undergo proliferation and secrete a collagen type 1-rich extracellular matrix. In the next phase, cellular proliferation decreases, and the cells express factors involved in matrix maturation such as alkaline phosphatase. In the final stage, osteoblasts initiate matrix mineralization and express factors such as integrin-binding sialoprotein and osteocalcin (3–5).

Osteoblast differentiation is tightly coordinated by the activities of transcriptional regulators; these include the master transcription factors RUNX2 and osterix (OSX),[2] which govern the expression of genes involved in the developmental process (6). RUNX2 is indispensable for skeletal development and controls osteoblast differentiation by regulating the commitment of osteoprogenitors and activating major bone matrix genes (7). Osterix is also necessary for osteoblast differentiation and bone formation and functions downstream of RUNX2 (6). Other transcription factors with roles in osteoblasts include MSX2, DLX5, TWIST-1, AP1, ATF4, HOXA10, and ZFP521 (6–9).

Dimethyl sulfoxide (DMSO; $(CH_3)_2SO$) is a small amphipathic molecule that is widely used as a solvent due to its abilities to dissolve both polar and nonpolar compounds (10). Currently, DMSO is used as a cryo-preserving agent in cell banking (11) commonly at 10% concentrations that are then injected directly into the patient. Notably, DMSO is reported to stimulate osteoblast differentiation in MC3T3-E1, a mouse pre-osteoblast cell line, through ERK activation of transcription factors Runx2 and osterix (12).

In this study, we show that DMSO acts as a potent enhancer of human and mouse osteoblast differentiation as demonstrated by the significant gains in alkaline phosphatase (ALP) activity and mineralization observed throughout differentiation. Significantly, the effects of DMSO were anabolic in nature,

* This work was supported by grants from the National Health and Medical Research Council of Australia (to N. A. M.) and the Australian Research Council (to D. W. H.).

[1] To whom correspondence should be addressed. Tel.: 61-7-55528330; Fax: 61-7-55528908; E-mail: n.morrison@griffith.edu.au.

[2] The abbreviations used are: OSX, osterix; ALP, alkaline phosphatase; OM, osteogenic medium; α-MEM, minimum essential medium; VD3, 1,25-dihydroxyvitamin $D_3$; qPCR, quantitative PCR; ECM, extracellular matrix.

such that the extent of matrix mineralization in DMSO-treated cells was greater than that of nontreated control cells, even when experiments were continued to the point where all cells were terminally differentiated. DMSO-enhanced osteoblast differentiation was used, in the model cell line MC3T3-E1, to identify novel genes involved in the developmental process. Unexpectedly, *Mef2c* was the transcription factor most potently induced by DMSO. *Mef2c* is a MADS-box transcription factor that is most commonly associated with the development and differentiation of the heart and skeletal muscle (13). Here, we show that *Mef2c* gene expression is dynamically regulated during osteoblast differentiation and that shRNA-mediated *Mef2c* gene silencing is associated with highly significant decreases in ALP activity, osteoblast gene expression, and matrix mineralization, demonstrating a critical role for Mef2c in osteoblast differentiation.

## MATERIALS AND METHODS

*Cell Culture and Osteoblast Differentiation*—MC3T3-E1 cells (subclone 14) were maintained in minimum essential medium ($\alpha$-MEM) (Invitrogen) containing 10% fetal bovine serum (FBS, Invitrogen), 1% penicillin/streptomycin solution (Invitrogen), and 1 mM sodium pyruvate (Invitrogen); this medium augmented with 50 $\mu$g/ml ascorbic acid and 10 mM $\beta$-glycerophosphate was termed osteogenic medium (OM). For osteoblast differentiation, cells were seeded in 24-well culture plates at a density of $2.5 \times 10^4$ cells/well in a total volume of 0.5 ml of medium, and then at 48 h, medium was replaced with OM with various concentrations of DMSO. Medium was changed every 72 h unless stated otherwise. For calvarial osteoblast differentiation, calvaria obtained from newborn mice were rinsed in phosphate-buffered saline (PBS) and digested four times sequentially with 0.1% collagenase A and 0.2% dispase II (Roche Applied Science) in PBS to liberate embedded cells. The pooled digestion solution was passed through a 70-$\mu$m cell strainer, and cells were recovered via centrifugation. The cells were seeded into culture flasks containing $\alpha$-MEM and grown for 3–4 days prior to osteoblast differentiation. Calvarial cells were prepared for osteoblast differentiation as per MC3T3-E1 cells. Human primary osteoblasts were obtained from biopsy material donated at orthopedic procedures; bone was minced and washed in PBS, removing marrow and adipocytes, and then treated with trypsin (Invitrogen) for 5 min. Pieces were then washed in PBS and osteoblasts permitted to grow out from explants in $\alpha$-MEM with 10% FBS (Invitrogen). Mineralization and ALP assays were done as for MC3T3-E1 cells. Adipocyte-derived mesenchymal cells were obtained from 2-h collagenase digestion at 37 °C of excised and minced fat pads. Cells were washed in PBS and cultured in Dulbecco's modified Eagle's medium (DMEM) with 5% FBS. 293T cells were maintained in DMEM containing 10% FBS (Invitrogen) and 1% penicillin/streptomycin solution (Invitrogen). All cells were maintained at 37 °C in a humidified atmosphere with 5% $CO_2$. DMSO concentrations were presented as percent volume. Procedures involving human samples were approved by the institutional committee at Queensland University of Technology. Procedures involving mice were approved by the animal ethics committee of Griffith University.

*Alkaline Phosphatase Activity and Matrix Mineralization Assays*—ALP activity was assessed via the spectrophotometric quantitation of *p*-nitrophenol generated through the hydrolysis of *p*-nitrophenyl phosphate. Briefly, cells were washed with 1 volume of PBS and lysed with the addition of 200 $\mu$l of 50 mM Tris-HCl, pH 8.0, and 0.5% Triton X-100 (per well, 24-well plate). 10 $\mu$l of cell lysate was incubated with 200 $\mu$l of 1 M diethanolamine, 0.5 mM $MgCl_2$, pH 9.8, containing 10 mM *p*-nitrophenyl phosphate for 15–30 min. The reaction was stopped by the addition of 50 $\mu$l of 3 M NaOH, and the absorbance was measured at 405 nm. Enzyme activity was standardized using purified calf intestinal ALP (New England Biolabs) and normalized to protein content as measured by the DC protein assay kit (Bio-Rad). ALP activity was expressed as nanomoles of *p*-nitrophenyl phosphate converted per min per mg of protein (nanomoles/min/mg protein). Matrix mineralization was assessed using Alizarin Red S staining according to Gregory *et al.* (14). Units are absorbance of solubilized Alizarin Red S measured at 405 nM per culture well. One $A_{405}$ unit represents 2.96 $\mu$mol of Alizarin Red S precipitated per culture.

*RNA Extraction and cDNA Synthesis*—RNA was extracted from cells using the acid guanidinium thiocyanate/phenol/chloroform method (15). For cDNA synthesis, ~1 $\mu$g of total RNA was treated with DNase I (Sigma) to remove any residual DNA and converted to cDNA using the ImProm-II reverse transcription system (Promega) according to the manufacturer's instructions. Reactions were carried out in 20-$\mu$l volumes, and all cDNA samples were diluted 1:5 in DNase-free water prior to real time PCR.

*Primers and Quantitative PCR (qPCR)*—PCR primers used in the study are listed in Table 1 and were designed from DNA sequences available through the Entrez Nucleotide database. Mouse gene nomenclature conventions were used (protein indicated by roman type and gene names in italic type). The specificities of candidate primer pairs were assessed by BLAST and BLAT analyses. Primer pairs were selected that gave single amplification products using *in silico* PCR. Specificity of amplification was verified by acrylamide gel electrophoresis, revealing a single fragment of the predicted size. qPCR amplifications were performed in an iCycler iQ real time PCR detection system (Bio-Rad) using the iQ SYBR Green supermix (Bio-Rad). Reactions were carried out in total volumes of 20 $\mu$l and included 250 nM of each primer and 2 $\mu$l of diluted cDNA template containing 100 ng of cDNA. The thermal cycler conditions were as follows: step 1, 95 °C for 90 s; step 2, 95 °C for 10 s, 59 °C for 10 s, and 72 °C for 25 s (45 cycles); step 3, melt curve analysis from 59 to 95 °C in 0.5 °C increments. The specificity of the individual amplifications was assessed by the examination of the melt curves to confirm the presence of single gene-specific peaks of the characteristic melting temperature. Gene expression levels were normalized to the normalization factor generated by the average of *Actb, B2m, Hmbs,* and *Hprt1* internal control genes as determined by the GeNorm algorithm of Vandesomple *et al.* (16). Transcript levels are presented as fold change compared with zero time base-line levels.

*Microarray Analysis*—Affymetrix and Illumina GeneChip microarray analysis was conducted at the Australian Genome Research Facility, Melbourne, Australia. For each sample, total

**TABLE 1**
**Real time qPCR primers used in the study and oligonucleotide sequences of Mef2c targeting shRNAs**

| Name | Accession no. | Forward (5′–3′) | Reverse (5′–3′) |
|---|---|---|---|
| **Genes** | | | |
| *Ibsp* | NM_008318 | gcgtcactgaagcaggtg | cggtaagtgtcgccacgag |
| *Mef2c* | NM_025282 | gctgagatacgcttagcacttgagt | cgggtctgtccaaacctctataca |
| *Osc* | NM_001032298 | gcagacaccatgaggaccc | ggtctgatagctcgtcacaagc |
| *Osx* | NM_130458 | tggaatgtaccccagtcctctcgac | ccaggccttgcacatattaagcatt |
| *Runx2* | NM_009820 | cagtcacctcaggcatgtc | gcgtgctgccattcgag |
| *Runx2-II* | NM_009820 | ccaggaagactgcaagaagg | tattcctgcatggactgtggtt |
| *Actb* | NM_007393 | ctctggctcctagcaccatgaaga | gtaaaacgcagctcagtaacagtccg |
| *B2m* | NM_009735 | ctgctacgtaacacagttccaccc | catgatgcttgatcacatgtctcg |
| *Hmbs* | NM_013551 | gagtctagatggctcagatagcatgc | cctacagaccagttagcgcacatc |
| *Hprt1* | NM_013556 | gaggagtcctgttgatgttgccag | ggctggcctataggctcatagtgc |
| *Dpt* | NM_001937 | agatatacaccagcagacccaacag | catgggaaagggagaattatccttc |
| *Sost* | NM_024449 | caaccagtcggagctcaaggactt | agtagagaccgcaggtccttctgc |
| **shRNAs** | | | |
| Sh1 | 531–549[a] | gatccgaatagtatgtctcctggtttcaagagaa ccaggagacatactattcttttttg | aattcaaaaagaatagtatgtctcctggttctct tgaaaccaggagacatactattcg |
| Sh2 | 682–700 | gatccggtaacctgaacaagaatattcaagagat attcttgttcaggttacctttttg | aattcaaaaaggtaacctgaacaagaatatctct tgaatattcttgttcaggttaccg |
| Sh3 | 236–254 | gatccggacaaactcagacattgtttcaagagaa caatgtctgagtttgtcctttttg | aattcaaaaaggacaaactcagacattgttctct tgaaacaatgtctgagtttgtccg |

[a] Numbers indicate the nucleotide distance from the ATG start codon of Mef2c mRNA (NM_025282). The following gene abbreviations are used: *Ibsp*, integrin-binding sialoprotein; *Mef2c*, myocyte enhancer factor 2C; *Osc*, osteocalcin or bone γ-carboxyglutamate protein 2; *Osx*, osterix or trans-acting transcription factor SP7; *Runx2, runt*-related transcription factor 2; *Actb*, β-actin; *B2m*, $\beta_2$-microglobulin; *Hmbs,* hydroxymethylbilane synthase; *Hprt1*, hypoxanthine-guanine phosphoribosyltransferase; *Dpt*, dermatopontin; *Sost*, sclerostin.

RNA (10 μg) underwent quality assessment by running a sample through an Agilent BioAnalyzer prior to microarray processing and scanning.

*Immunohistochemistry*—C57BL/6J mice were either day 15 fetal or week 12 adult. Tissues were fixed in 4% paraformaldehyde/PBS, decalcified in 0.5 M EDTA for 2 weeks, and embedded in paraffin. Five-micrometer sections were prepared for immunohistochemistry. Slides were blocked with 1% FBS for 10 min, then incubated for 2 h at 21 °C with rabbit anti-MEF2C primary antibody (Abcam, 64644) diluted 1:100 in buffered saline at a final concentration of 9 μg/ml or with a nonimmune rabbit IgG (Santa Cruz Biotechnology) using the same final concentration, followed by rinses and addition of a biotinylated goat anti-rabbit IgG (Santa Cruz Biotechnology) for 30 min at room temperature. After incubation with streptavidin-horseradish peroxidase (DAKO) for 30 min at room temperature, slides were stained by exposure to β-diaminobenzidine-liquid chromogen (DAKO) followed by counterstaining with Mayer's hematoxylin and mounted in Cytoseal 60 (Richard Allan Scientific). Positive antibody staining was identified by the presence of brown color.

*shRNA Constructs, Retroviral Particle Production, and Infection—Mef2c* shRNA sequence 1 (Sh1) was described previously (17). Sh2 and Sh3 were designed using the Promega siRNA Target Designer (version 1.51) in the mouse *Mef2c* mRNA. Sequence specificities were assessed via BLAST analysis. Forward and reverse oligonucleotides encoding the shRNA sequences (Table 1) were annealed via thermal cycling and cloned into the BamHI and EcoRI sites of pSIREN-RetroQ (Clontech). The pSIREN-RetroQ Luc vector (Clontech), which targets firefly luciferase, was used as a control. Retroviral particle production was performed by co-transfection of pSIREN-RetroQ vectors, the VSV-G envelope glycoprotein vector pCSIG, and the Friend murine leukemia virus-based Gag-Pol expression vector pC57GP (18) in 293T cells using FuGENE HD transfection reagent. Fresh medium was added to cells 24 h post-transfection, and viral supernatants were harvested 48 h later. Viral supernatants were passed through a 0.45-μm pore size filter and used directly for infections. Infections were performed by seeding MC3T3-E1 cells at $2.5 \times 10^5$ cells in 25-$cm^2$ culture vessels. 24 h later, the medium was replaced with viral supernatant containing 8 μg/ml Polybrene. 24 h later, infected cells were selected by replacing the viral supernatant with fresh medium containing 4 μg/ml puromycin. Infected cells were expanded in culture prior to use for subsequent analyses. Transient transfections were done using FuGENE (Roche Applied Science) according to the manufacturer's protocol. Mef2c expression vector was constructed in pBABE vector (Addgene) using mouse *Mef2c* coding region amplified from MC3T3-E1 cDNA. pOSLUC was made by inserting the 600 bp of human osteocalcin promoter upstream of firefly luciferase in the pGL-Basic vector (Promega). This construct contains Runx2, osterix, and vitamin D receptor-binding sites. *Renilla* luciferase was used as a control for transfection efficiency according to the Dual-Glo procedure (Promega). Phosphorylation status of kinases was assayed using RayBio Phospho-ELISA kits exactly according to the manufacturer's instructions.

*Cellular Proliferation Assays*—Cellular proliferation was assessed using the 3-(4,5-dimethylthiazol-2-yl)-2,5-diphenyltetrazolium bromide method. MC3T3-E1 cells were seeded at $1 \times 10^4$ cells per well in 24-well culture plates and grown in osteogenic medium for 1–7 days. Cultures were gently washed once with warm PBS, and fresh medium containing 3-(4,5-dimethylthiazol-2-yl)-2,5-diphenyltetrazolium bromide to a final concentration of 0.5 mg/ml was added to the wells. After an incubation period of 3 h, medium was removed, and the dye was solubilized via the addition of 200 μl of isopropyl alcohol containing 0.1% SDS and 0.04 N hydrochloric acid. The absorbance of the dye solution was measured at 570 nm.

*Statistical Analysis*—ALP activity, ECM mineralization, and cellular proliferation assays were assessed using Student's *t* test or analysis of variance with LSD post hoc tests. Analysis of variance of natural log-transformed gene expression data with LSD post hoc tests was used to assess the significance of differ-

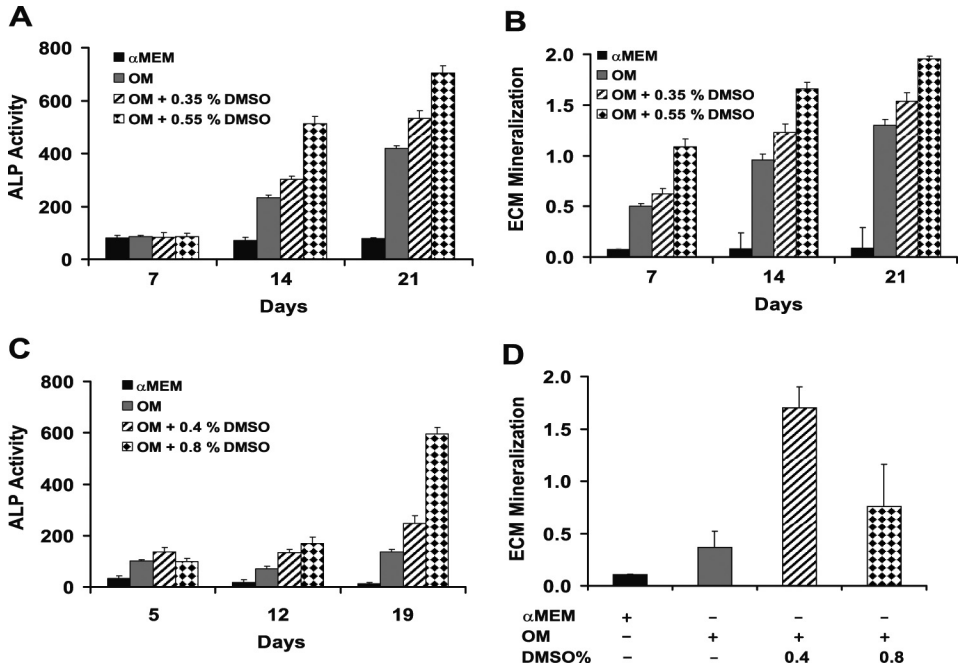


FIGURE 1. **DMSO enhances ALP activity and ECM mineralization in osteoblasts.** Cultured human osteoblasts were grown for the times shown in α-MEM (*black columns*), osteogenic medium (*gray columns*), or OM supplemented with DMSO (*striped* and *checked columns*) and assessed for ALP activity (*A*) and ECM mineralization (*B*). Mouse adipocyte-derived mesenchymal cells were cultured in a similar manner with similar results, including increased ALP activity (*C*) and increased mineralization associated with DMSO treatment at the concentrations indicated (*D*). Data represent mean ± S.E. of at least three independent samples.

ences between means. For time course analysis, the generalized linear model (SPSS) was used. Cycle threshold corrected for housekeeper genes was considered a normally distributed trait and used for statistical analysis. Significant differences were denoted by $p < 0.01$. Error bars in graphs represent a standard error. In some cases where effects are obvious and substantial, $p$ values are not presented.

## RESULTS

*DMSO Promotes Osteoblast Differentiation*—Primary human osteoblasts were cultured in OM supplemented with increasing concentrations of DMSO, resulting in increased ALP activity (Fig. 1*A*) and enhanced mineral formation as detected using Alizarin Red staining (Fig. 1*B*). Similarly, mouse mesenchymal cells, derived from testicular fat pads cultured in OM, exhibited a similar dose response of increased ALP activity and enhanced mineralization to DMSO supplementation (Fig. 1, *C* and *D*, respectively).

The response of the pre-osteoblast model cell line, MC3T3-E1, to DMSO was characterized in detail for the dose response of ALP activity and mineralization (at 12 days, Fig. 2, *A* and *B*, respectively) and time course of response at 0.55% DMSO (Fig. 2, *C* and *D*, respectively). Enzyme activity levels were maximally induced (2.9-fold) at 0.55% DMSO and gradually decreased at the two higher doses of 0.8 and 1.0%, while still significantly elevated compared with control. In parallel, a highly significant dose-dependent increase in ECM mineralization was also observed in response to DMSO treatment (Fig. 2*B*). The rise in mineralization paralleled ALP activity. As expected, mineralization was not detected over the first 5 days of differentiation for either treatment group. By 7 days, small amounts of mineralization were detectable in both groups with levels slightly greater in DMSO-treated cells. Beyond that time, DMSO-treated cells contained significantly more mineral than control cells at every time point and culminated in a 2.4-fold increase by day 21. These data indicated that DMSO exerted an anabolic effect on MC3T3-E1 osteoblast differentiation where cells contained significantly increased levels of ALP enzyme activity and deposited greater amounts of mineral in response to treatment.

Exposure of cells in OM to DMSO for the first 3 days of culture was sufficient for the maximal enhanced mineralization effect, as delayed addition did not result in increased mineralization (Fig. 2*E*). These data suggest a critical early time window of effect of DMSO on MC3T3-E1 cells. In the first 2 days DMSO did not have a significant effect on cellular proliferation; however, a minor suppression became apparent at 3 days that persisted as cells differentiated under the effect of DMSO and OM (Fig. 2*F*).

A critical early window of exposure to DMSO was observed, although the full mineralization effect in MC3T3-E1 cells developed over several days after this critical window. If DMSO had a direct inducing effect on bone-specific promoters, increased gene induction might be expected within that 72-h window. This was tested by transfecting a human osteocalcin promoter-luciferase construct into MC3T3-E1 cells and culturing in OM for 48 h. DMSO (2.5%) exposure was limited to the last 24 h prior to harvest (at 72 h after transfection) and assay to minimize effects on proliferation and focus on transcription effects. Two known inducers of human osteocalcin, 1,25-dihydroxyvitamin $D_3$ (VD3, 100 nM) treatment and Runx2 expression vector co-transfection, were used as positive controls. VD3 activation depends on endogenous vitamin D receptor. As expected, VD3 induced the human osteocalcin promoter. In

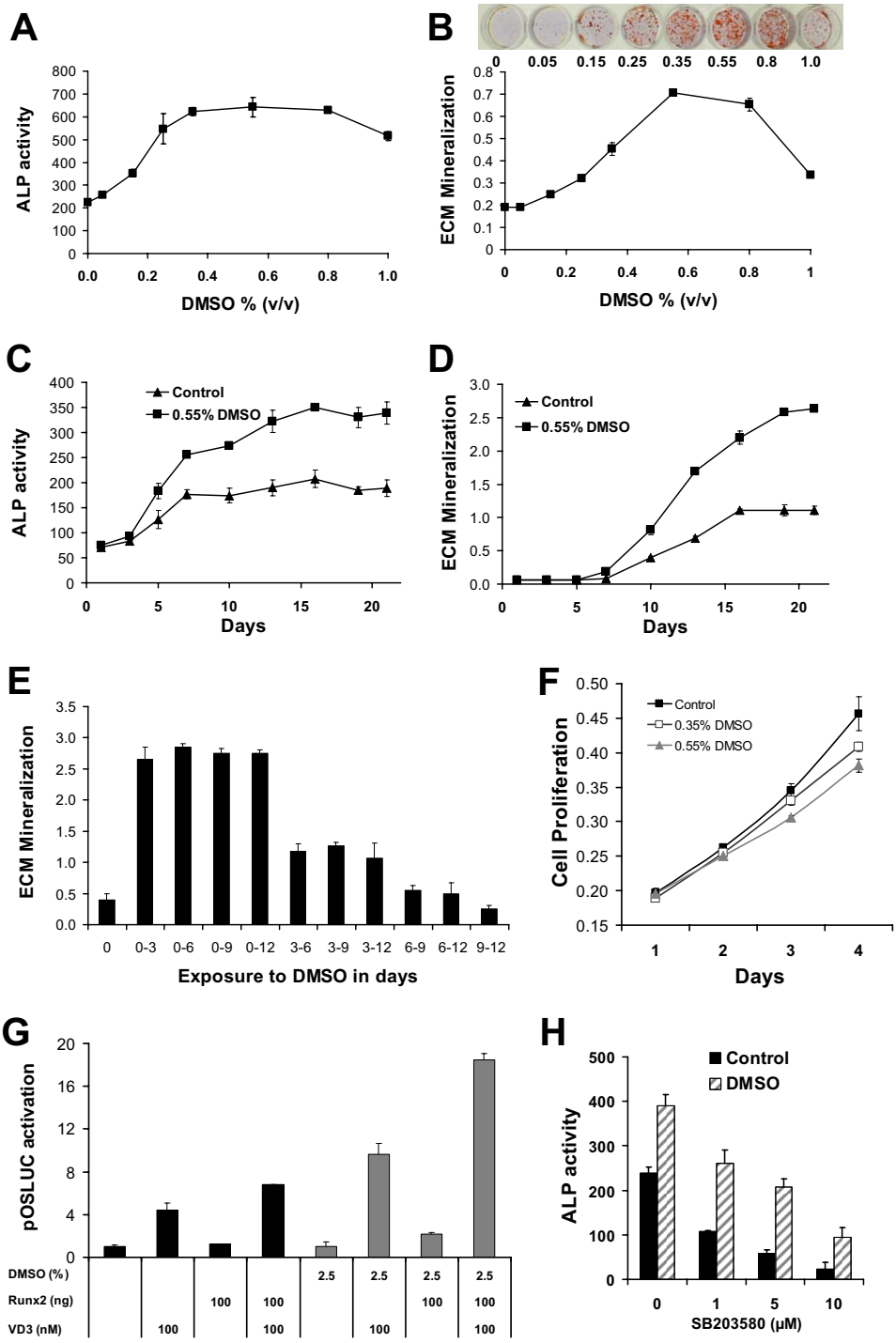


FIGURE 2. **DMSO enhances ALP activity and ECM mineralization of a model osteoblast cell line (MC3T3-E1).** Differentiating MC3T3-E1 cells were treated with various concentrations of DMSO and assessed for ALP activity (*A*) and ECM mineralization (*B*). *Inset photo* in *B* shows mineral nodule formation, visualized using Alizarin Red S, with increasing DMSO at day 12. Levels of ALP activity (*C*) and ECM mineralization (*D*) are shown during osteoblast differentiation time courses in control cultures (OM medium, *black triangles*) and OM plus DMSO-treated cells (0.55% DMSO, *black squares*). The time of exposure of cells to DMSO altered the mineralization outcome (*E*), with the first 3 days of culture being critical for the maximal effect of DMSO. *F,* cell proliferation was only mildly suppressed by DMSO; MC3T3-E1 cells were seeded at $1 \times 10^4$ cells per well in 24-well culture plates and treated with various concentrations of DMSO. The cells were grown over a period of 4 days, and cellular proliferation was assessed on each day via the 3-(4,5-dimethylthiazol-2-yl)-2,5-diphenyltetrazolium bromide method. *G,* DMSO treatment in OM results in increased induction of transfected human osteocalcin promoter within the first 72 h of exposure; human osteocalcin promoter driving luciferase (pOSLUC) was transfected into MC3T3-E1 cells and induction measured after 72 h in OM alone (*black columns*) or OM with exposure to DMSO for the last 24 h (*gray columns*). Treatments included co-transfection of 100 ng of Runx2 expression vector and/or treatment with 100 nM VD3 to induce the osteocalcin promoter. *H,* DMSO enhancement of ALP activity in MC3T3-E1 is resistant to the p38 MAPK inhibitor SB203580. Enhancement by DMSO still occurred from the lower basal level that results from inhibition of p38 MAPK pathway by SB203580. Cell culture was 12 days. *Error bars* are ± S.E. of at least three independent samples. *p* values are omitted because effects are large.

the absence of DMSO, maximal expression was seen with VD3 and Runx2 treatment (6.8-fold). In the presence of DMSO, a significant boost to induction was seen, up to 18.5-fold ($p < 10^{-9}$, see Fig. 2*G*). An increase in osteocalcin induction in MC3T3-E1 cells after 24 h of exposure to DMSO treatment (in OM) is consistent with additional transcription factors being available to enhance promoter activity.

Quantitative assays for the phosphorylation status of protein kinases across the first 30 h in OM plus DMSO compared with OM found no convincing involvement of DMSO in ERK1/2, p38 MAPK, and JNK signaling pathways. Significant increases in phosphorylated signaling factors were seen after 30 h, with 2.8-fold ($p = 4.8 \times 10^{-7}$), for phospho-JNK, 1.8-fold ($p = 7.8 \times 10^{-5}$) for phospho-ERK, and only 1.4-fold ($p = 8.6 \times 10^{-6}$) for phospho-p38 MAPK. Significant effects of DMSO on phosphorylated kinases were observed for ERK ($p = 0.009$) and JNK ($p = 0.014$); however, these were only minor decreases in DMSO-treated cells (10 and 7% decreases for ERK and JNK, respectively). There were no significant effects on total kinase content between OM and OM plus DMSO treatments at any time point for ERK1/2, p38 MAPK, or JNK (data not shown), although total kinase increased over time. Finally, we considered if the pool of phosphorylated kinase over total kinase changed according to DMSO; once again there were no significant DMSO-related changes within 30 h. Furthermore, experiments with inhibitors of these pathways at appropriate concentrations did not suggest a role for the following inhibitors and pathways in the DMSO effect: U0126 for the ERK1/2 pathway, SB203580 for the p38 MAPK pathway, and Ly-294002 for the PI3K/AKT pathway. The p38 MAPK inhibitor SB203580 is reported to inhibit osteoblast gene activation through phosphorylation of osterix (19). Consistent with this observation, SB203580 decreased ALP activity in a dose-dependent manner in MC3T3-E1 cells grown in OM; however, the DMSO enhancement was still proportional to the reduced ALP activity (Fig. 2*H*). Taken together, these data suggest that the initial effects of DMSO action in osteoblasts occur in a critical 72-h window and may involve enhanced induction of osteocalcin at the transcriptional level (based on promoter transfection), but it seems unlikely to involve p38 MAPK, ERK1/2, JNK, or PI3K/Akt at least within the first 30 h. Those effects observed were either in the reverse sense to a DMSO-mediated enhancement effect or were minor enough in magnitude as to be discounted.

*DMSO Treatment Is Associated with Increased Expression of Osteoblast Markers*—DMSO was clearly able to enhance osteoblast differentiation as revealed by elevated ALP activity and mineralization. We next set out to investigate the effects of DMSO on osteoblast gene expression. Accordingly, the expression of marker genes was assessed at multiple time points throughout osteoblast differentiation. Cells were grown in osteogenic conditions over a period of 19 days and were harvested for qPCR analysis of endogenous gene expression at numerous time points (Fig. 3). Gene expression was expressed as fold change in transcript levels, measured by qPCR, referenced to zero time.

Transcript levels for endogenous mouse osteocalcin (mouse gene *Bglap2*) were approximately doubled by DMSO treatment, reaching a peak at day 7 (Fig. 3*A*). Similar changes were seen in integrin-binding sialoprotein (*Ibsp*, Fig. 3*B*), matrix metalloproteinase 13 (Fig. 3*C*), and the osteoclast differentiation factor, receptor activator of NFκB ligand (*Rankl*, Fig. 3*D*). Not all extracellular matrix protein genes were induced by DMSO; dermatopontin (*Dpt*) was potently repressed by DMSO (Fig. 3*E*). The expression of osteoblast transcription factor, osterix (*Osx*, Fig. 3*F*), was significantly increased by DMSO treatment at 3 days and showed increased transcript levels at later time points, suggesting that DMSO treatment results in an early and sustained increase in a key osteoblast-specific transcription factor. The up-regulation of osterix within 3 days may be sufficient to explain DMSO-enhanced osteocalcin promoter activity in transfection (Fig. 2*G*), and the continued up-regulation of osterix over 21 days may be sufficient to explain enhanced mineralization; further work is required to directly test such hypotheses. *Runx2* transcript levels were not significantly different at early time points between DMSO-treated and control cells, and although *Runx2* transcript levels were higher in DMSO-treated cells as *Runx2* increased over time, this was only nominally significant ($p = 0.03$) at one time point (Fig. 2*G*).

*Identification of Genes Super-induced by DMSO via GeneChip Expression Analysis and Verification by qPCR*—Differentiating MC3T3-E1 cells treated with DMSO clearly produced significantly greater amounts of mineralized matrix. One of the potential uses of DMSO-enhanced mineralization was to search for genes overexpressed as a consequence of DMSO treatment, effectively serving as a screening tool to identify novel genes involved in osteoblast differentiation and function. To search for genes super-induced by DMSO, we used Affymetrix GeneChip microarrays to quantify gene expression in MC3T3-E1 cells grown under three different experimental conditions as follows: standard medium that did not induce differentiation (nonmineralizing control); osteogenic medium that induced ECM mineralization (OM); and osteogenic medium supplemented with DMSO that produced highly mineralized matrix (OM plus DMSO). Cells were harvested for RNA extraction after 12 days of culture; this time point was chosen because four of five osteoblast-expressed genes (*Osx*, *Ibsp*, *Mmp13,* and osteocalcin) were significantly elevated as a consequence of DMSO treatment as reported above.

To identify DMSO super-induced genes, we applied two search filters to the microarray gene expression data. First, all the genes that were at least moderately expressed (signal intensity over 100) and induced by more than 3-fold in OM relative to control were selected. These genes were further filtered by selecting only those that were further increased more than 1.5-fold by DMSO. The filtering process resulted in the identification of 28 genes super-induced by DMSO (Table 2). DMSO treatment resulted in the super-induction of genes known to participate in bone biology such as osteoprotegerin (*Tnfrsf11b*) and the integrin-binding sialoprotein (*Ibsp*). Because osterix was induced by DMSO (Fig. 3*F*), we reasoned that any other transcription factor that is up-regulated by DMSO in mineralizing MC3T3-E1 cells is a candidate for an osteoblast transcription factor with a role in mineralization. *Mef2c* transcription factor was identified as a DMSO super-induced gene on array.

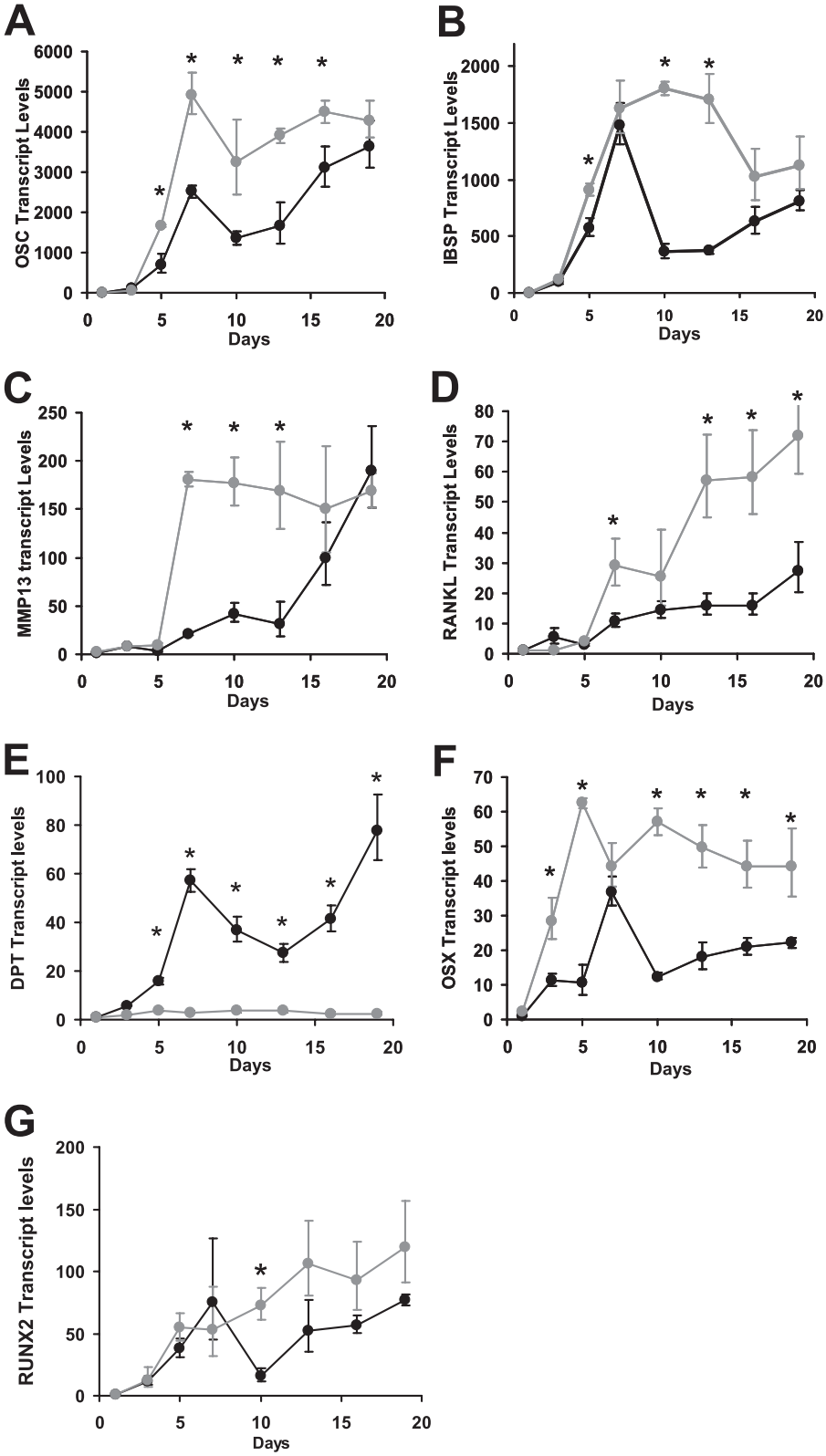


FIGURE 3. **DMSO significantly increases the expression of osteoblast markers during differentiation.** Osteogenic medium (*black circles, black line*) was compared with OM plus 0.55% DMSO (*gray circles, gray line*). MC3T3-E1 cells were harvested at various time points during osteoblast differentiation for quantitative gene expression analysis of osteocalcin (*OSC*, *A*), integrin-binding sialoprotein (*IBSP*, *B*), matrix metalloproteinase 13 (*MMP13*, *C*), and receptor activator of NFκB ligand (*RANKL*, *D*). Remarkably, dermatopontin (*DPT*, *E*) was completely repressed by DMSO in osteogenic medium, in comparison with OM control. The osteoblast transcription factor osterix (*F*) was significantly induced by DMSO at most time points assessed, including 3 days. *Runx2* (*G*) was not significantly different early in DMSO treatment, and although of greater magnitude in DMSO-treated cells, it was significantly different with respect to DMSO at day 10 only (*asterisk*, $p = 0.03$). Data represent mean ± S.E. of three independent samples. *A–F, asterisks* denote significantly different from OM (for that time point) at $p < 0.01$. Overall $p$ values (not shown for each) of the treatment effect for DMSO were determined using the general linear model-based analysis of variance, and all were $<10^{-6}$, except for *Runx2* (*G*), which was not significant.

**TABLE 2**

**Genes super-induced by DMSO in differentiating osteoblasts**

Results are shown as fold change in gene expression. Cells were cultured for 12 days post-induction of osteogenic differentiation. CT indicates control cells cultured in nonmineralizing medium; OM, cells cultured in osteogenic medium; DMSO, cells cultured in osteogenic medium supplemented with DMSO.

| Accession no. | -Fold change OM/CT | -Fold change DMSO/CT | -Fold change DMSO/OM | Gene name | Gene |
|---|---|---|---|---|---|
| D17444.1 | 3.2 | 15.0 | 4.7 | Soluble D-factor/LIF receptor | *Lifr* |
| NM_028943 | 14.0 | 54.9 | 3.9 | Sphingomyelin synthase 2 | *Sgms2* |
| NM_025282.1 | 5.5 | 21.1 | 3.8 | Myocyte enhancer factor 2C | *Mef2c* |
| NM_013703.1 | 6.5 | 24.6 | 3.8 | Very low density lipoprotein receptor | *Vldlr* |
| AK003671.1 | 27.7 | 100 | 3.7 | Carbonic anhydrase 3 | *Car3* |
| NM_080440 | 9.3 | 32.3 | 3.5 | Solute carrier family 8 (sodium/calcium exchanger), member 3 | *Slc8a3* |
| AB013898.1 | 3.1 | 10.5 | 3.5 | Osteoclastogenesis inhibitory factor | *Tnfrsf11b* |
| BC004048.1 | 9.4 | 32.2 | 3.4 | Wnt inhibitory factor 1 | *Wif1* |
| BB042892 | 5.7 | 19.0 | 3.3 | Ubiquitin-conjugating enzyme 8 | *Ubce8* |
| BE370703 | 8.4 | 27.7 | 3.3 | Neutrophil cytosolic factor 1 | *Ncf1* |
| NM_153060 | 5.8 | 16.3 | 2.8 | Spinster homolog 2 | *Spns2* |
| BM240191 | 3.6 | 10.1 | 2.8 | Rho-associated coiled-coil forming kinase 1 | *Rock1* |
| BI964347 | 3.3 | 8.6 | 2.6 | A disintegrin and metalloproteinase domain 12 (meltrin-$\alpha$) | *Adam12* |
| XM_907370 | 4.3 | 11.2 | 2.6 | Collagen, type XXII, $\alpha$1 | *Col22a1* |
| NM_021491 | 3.6 | 8.7 | 2.4 | Sphingomyelin phosphodiesterase 3 | *Smpd3* |
| NM_172454 | 10.0 | 23.6 | 2. | Pannexin 3 | *Panx3* |
| NM_153170 | 4.1 | 9.7 | 2.3 | Solute carrier family 36 (proton/amino acid symporter), member 2 | *Slc36a2* |
| NM_001081064 | 3.7 | 8.0 | 2.2 | PDZ domain containing 2 | *Pdzd2* |
| L20232.1 | 21.2 | 42.8 | 2.0 | Bone sialoprotein | *Ibsp* |
| NM_009760 | 2.9 | 5.6 | 2.0 | BCL2/adenovirus E1B interacting protein 3 | *Bnip3* |
| NM_011356 | 29.0 | 56.5 | 2.0 | Frizzled-related protein | *Frzb* |
| NM_053083 | 3.0 | 5.8 | 1.9 | Lysyl oxidase-like 4 | *Loxl4* |
| NM_016894 | 3.9 | 7.4 | 1.9 | Receptor (calcitonin) activity modifying protein 1 | *Ramp1* |
| NM_009331 | 5.0 | 9.5 | 1.9 | Transcription factor 7, T-cell specific | *Tcf7* |
| NM_019738 | 3.8 | 7.2 | 1.9 | Nuclear protein 1 | *Nupr1* |
| NM_011199 | 4.1 | 6.9 | 1.7 | Parathyroid hormone receptor | *Pthr1* |
| NM_030888 | 3.4 | 5.6 | 1.6 | C1q and tumor necrosis factor-related protein 3 | *C1qtnf3* |
| NM_053088 | 32.6 | 52.4 | 1.6 | Interferon-induced transmembrane protein 5 | *Ifitm5* |

*Transcript Profiling of Mef2c during Osteoblast Differentiation*—To confirm the validity of the microarray results, we performed qPCR analysis in MC3T3-E1 cell experiments to verify the expressions of *Ibsp* and *Mef2c* (Fig. 4, *A* and *B*). Relative to the control cells cultured in $\alpha$-MEM, *Ibsp* expression was significantly induced 16- and 82-fold in OM and OM plus DMSO cultures, respectively, confirming the microarray. Similarly, *Mef2c* gene expression was up-regulated 10- and 60-fold in OM and OM plus DMSO samples, respectively, relative to control. *Mef2c* gene expression was assessed during a time course of MC3T3-E1 differentiation (Fig. 4*C*), showing that *Mef2c* expression levels increased during the initial stages of differentiation, peaking at day 7 before decreasing by day 13. *Mef2c* transcript levels are induced up to 100-fold by culture in mineralizing medium. In cells treated with DMSO, the peak of *Mef2c* induction was earlier (5 rather than 7 days), and induction was more sustained at later time points. In this respect, the DMSO effect on *Mef2c* induction in MC3T3-E1 cells was similar to that observed for osterix (see Fig. 3*F*).

The induction of *Mef2c* was confirmed in mouse primary osteoblasts. Mouse calvarial osteoblasts were isolated and cultured in OM in the presence of DMSO. Similar to the results in MC3T3-E1 cells, *Mef2c* was induced in calvarial osteoblasts during culture in OM compared with control medium (Fig. 4*D*), and *Mef2c* expression was further enhanced by DMSO. Furthermore, DMSO enhanced mineralization by calvarial osteoblasts (Fig. 4*E*). These data confirm the cell line MC3T3-E1 as a reasonable model for Mef2c effects in osteoblasts. Furthermore, to verify that *Mef2c* has effects on osteoblast biology that occur in a manner independent of DMSO, the following experiments represented in Figs. 6–9 were done completely in the absence of DMSO in culture.

*Mef2c Expression in Osteoblasts in Vivo*—Immunohistochemistry was used to detect Mef2c protein in mouse osteoblasts (Fig. 5). Positive staining was seen in 15-day fetal mouse skull (Fig. 5*A*) in the maxilla and mandible (Fig. 5, *B* and *C*), where staining was found in association with developing bone and was stronger than in adjacent Meckel's cartilage (Fig. 5*C*). Cells immediately adjacent to the bone surface were positive for Mef2c (Fig. 5*D*). In adult mouse bone, positive staining was found in the growth plate associated with hypertrophic chondrocytes and cells lining bone in the cancellous region (Fig. 5*E*). In adult femoral cortical bone, similar positive cells lining the bone surface were observed (Fig. 5*F*). Staining was also observed in osteocyte-like cells in lacunae in adult cortical bone (Fig. 5*G*).

*Mef2c Gene Silencing Results in Defective Osteoblast Differentiation—Mef2c* expression in MC3T3-E1 cells followed a similar pattern to that of osterix and was enhanced by DMSO, suggesting Mef2c as a candidate bone transcription factor. This was tested using a Mef2c expression vector transfected into MC3T3-E1 cells. *Mef2c* mRNA levels were increased, and significant increases in endogenous osteocalcin and *Isbp* transcript levels were observed (Fig. 6, *A*–*C*). In a separate transfection, cultured over 16 days, significantly increased mineralization was observed in *Mef2c*-transfected cells (Fig. 6*D*). Because *Mef2c* transfection elevated the expression of osteoblast genes, we would expect *Mef2c* knockdown to have the reverse effect if the expression of osteocalcin and *Ibsp* is dependent on *Mef2c*. *Mef2c* expression was selectively knocked down using shRNAi-mediated gene silencing. One published (17) and two novel shRNAi sequences targeting three separate regions of the *Mef2c* sequence were designed and cloned into pSIREN-RetroQ (Sh1, Sh2; and Sh3). An

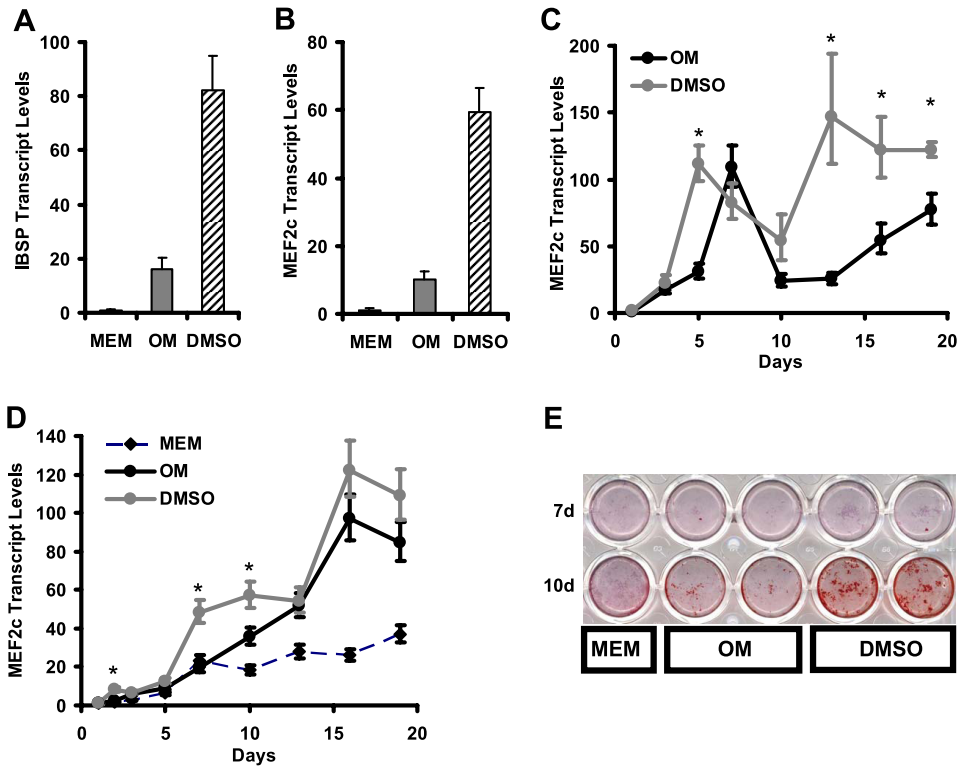


FIGURE 4. **DMSO treatment results in the super-induction of *Ibsp* and *Mef2c* gene expression in osteogenic medium (*A* and *B*, respectively).** Cells were grown in α-MEM (*MEM, black columns*), osteogenic medium (*OM*, *gray columns*), and osteogenic medium supplemented with 0.55% DMSO (*DMSO*, *striped columns*) for 12 days. Transcript profiling of *Mef2c* during osteoblast differentiation according to time (*C*) confirms sustained induction during osteoblast differentiation in OM (*black circles*) and super-induction by DMSO addition in OM (*gray circles*). *Mef2c* is induced during mouse calvarial cell cultures and shows super-induction with DMSO (*D*); *Mef2c* transcript levels were compared in calvarial osteoblasts grown in α-MEM (*MEM*, *back diamonds, striped line*), OM (*black circles, black line*), and OM plus 0.55% DMSO (*DMSO*, *gray circles, gray line*). *E* shows mineralization of mouse calvarial osteoblasts in α-MEM (*MEM*), OM, and OM plus 0.55% DMSO (*DMSO*) indicating enhancement of mineralization effect in calvarial osteoblasts by exposure to DMSO. *Asterisk* denotes significantly increased compared with OM ($p < 0.01$). Other *p* values omitted because effects are large (*A* and *B*). *d,* day.

shRNAi sequence targeting firefly luciferase mRNA was used as a control (Shlux). Pooled stably transfected MC3T3-E1 cell lines were generated via retroviral transduction and used in differentiation experiments.

Targeting of *Mef2c* transcripts with shRNA resulted in highly significant and consistent decreases in *Mef2c* expression levels throughout MC3T3-E1 osteoblast differentiation (Fig. 7*A*). The rank order of effectiveness of *Mef2c* shRNAs from least to most effective was Sh1, Sh2, and then Sh3. Although these knockdown cell lines had a slightly decreased rate of proliferation that was significant statistically (Fig. 7*B*), the magnitude of this effect was not large enough to explain observed biological effects. The impact of selectively reducing *Mef2c* expression levels on osteoblast differentiation was investigated. Targeting of *Mef2c* transcripts resulted in highly significant reduction in ALP activity (Fig. 7*C*), with one cell line, Sh3, showing almost total suppression. The accrual of mineral through the time course was dramatically suppressed (Fig. 7*D*), and a delay in the onset of visible bone nodule formation was observed (Fig. 7*E*). Highly significant reductions in mineral accrual occurred in all shRNA cell lines (Fig. 7, *D* and *E*) culminating in a 10-fold reduction by day 21.

The magnitude of decreased ALP activity was correlated to the potency of *Mef2c* silencing such that Sh3, which mediated the greatest reduction in *Mef2c* expression, produced the largest reduction in ALP activity, suggesting that ALP activity was dependent on *Mef2c* levels in the cells. However, suppression of mineralization appeared similar in all three knockdown cells lines.

*Knockdown of Mef2c Transcript Is Associated with Significant Decreases in Osteoblast Gene Expression*—Knockdown of *Mef2c* clearly resulted in reduced mineralization and ALP activity. To determine whether this was due to a block in osteoblast differentiation (where lack of induction of osteoblast-specific genes might be expected) or a block in mineralization due to the singular loss of ALP activity, gene expression of osteoblast marker genes was examined by qPCR. If Mef2c is necessary for the differentiation of osteoblasts, and acts as an osteoblast transcription factor, a flow on knockdown of osteoblast-related gene expression should be observed.

Osteoblast-related genes *Ibsp* and osteocalcin, which were up-regulated by DMSO, were strongly suppressed in anti-*Mef2c* shRNAi cell lines (Fig. 8, *A* and *B*, respectively), and in a manner related to the extent of *Mef2c* knockdown. Cell line Sh3 had the most potent knockdown, with almost complete suppression of *Ibsp* and osteocalcin gene expression and flow on knockdown of *Mmp13* (Fig. 8*C*). Recall that in DMSO-treated cells (see Fig. 3), dermatopontin (*Dpt*) transcript levels were suppressed by DMSO treatment (in which *Mef2c* expression was increased). In the Sh3 cell line, in which *Mef2c* is almost completely suppressed, a potent time-dependent induction of dermatopontin message was observed during culture in OM

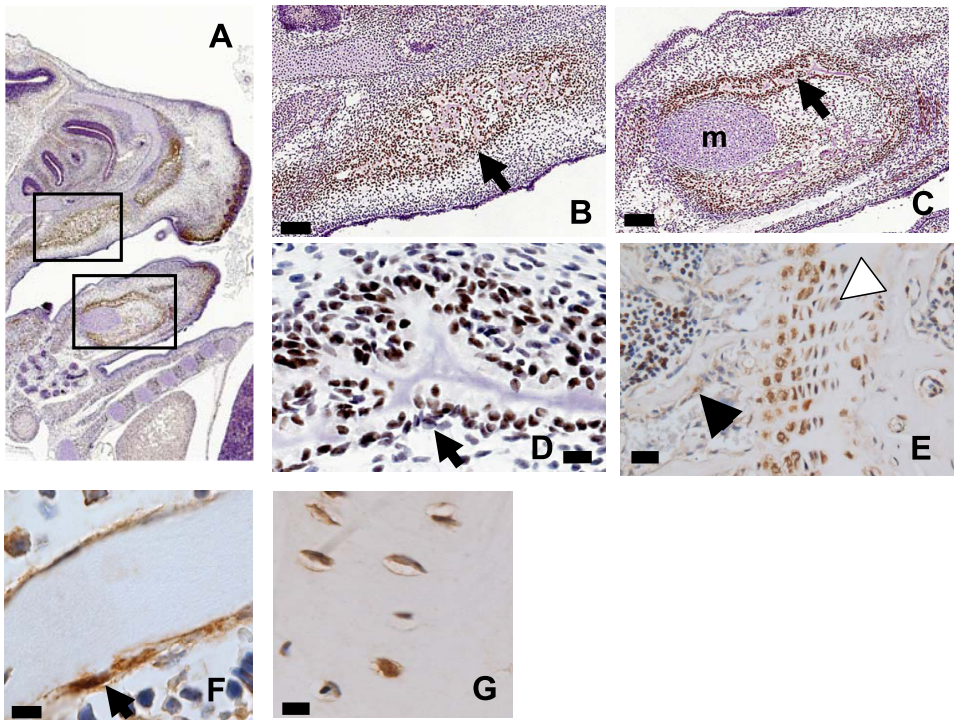


FIGURE 5. **Mef2c is present in osteoblasts.** *A,* immunohistochemistry of day 15 embryonic mouse head (parasagittal section, *A*), showing immunoreactivity (*brown* stain) in the mandible and the maxilla (*boxes*). *B* and *C, boxes* in image *A* are shown in greater detail; staining is positive in the maxilla (*B*) and the mandible (*C*). *Arrows* indicate examples of positive stain associated with developing bone; Meckel's cartilage is indicated (*m* in *C*). *Bars,* 200 μm. *D,* increased magnification of *arrow* location in *C* shows numerous positive staining cells around the developing bone (*bar,* 20 μm). *E,* analysis of adult mouse bone shows staining in the hypertrophic chondrocytes of the growth plate (*white arrow*) and in sites immediately adjacent to bone (*black arrow*). *Bar,* 100 μm. *F,* adult mouse cortical bones show bone lining cells stain positive for Mef2c. *G,* osteocytes in lacunae of cortical bone stain positive for Mef2c. *Bars, F* and *G,* 20 μm.

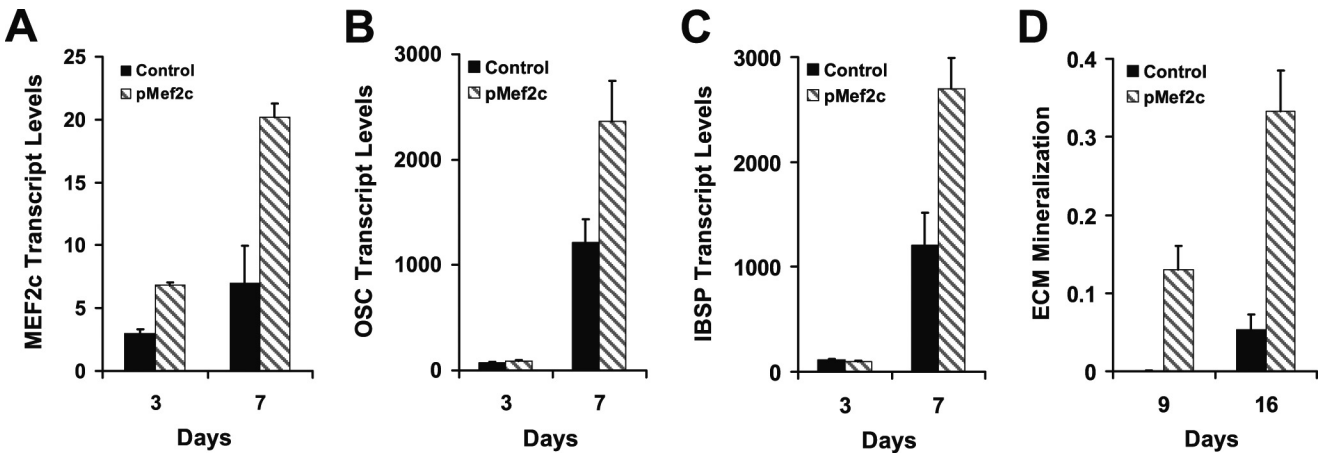


FIGURE 6. **Knock-in expression of *Mef2c* by transfection in MC3T3-E1 cells results in increased expression of *Mef2c* (*A*), osteocalcin (*OSC, B*), and integrin-binding sialoprotein (*IBSP, C*).** MC3T3-E1 cells were transfected and grown subsequently in OM for the specified time before harvest and assessment of mRNA levels by qPCR. All genes are significantly increased by *Mef2c* transfection at 7 days ($p < 0.001$). *D,* in a separate transfection experiment, cultured to 16 days, a significant increase in extracellular matrix mineralization was observed in *Mef2c*-transfected cells compared with empty vector transfected control ($p = 4 \times 10^{-4}$).

(Fig. 8*D*), suggesting *Mef2c* is a negative regulator of dermatopontin. These data suggest that *Mef2c* knockdown, at least in Sh3 cells line, results in the inverse phenotype to that of DMSO treatment as follows: inhibited mineralization coupled with a lack of ALP activity, failure to induce osteoblast marker genes, and a strong induction of *Dpt*. Flow on knockdown of osterix was significant in comparison with control Shlux to all knockdown cell lines (Sh1, $p = 0.02$; Sh2, $p = 0.02$, data not shown) and was strongest in Sh3 cell line ($p < 10^{-6}$, Fig. 8*E*). In Sh3 relative to Shlux, the knockdown of osterix was significant at all time points, including time 0 ($p = 1.0 \times 10^{-4}$). Flow on knockdown of *Runx2* ($p = 0.004$, Fig. 8*F*) was observed in Sh3; such flow on knockdown suggests that Mef2c is upstream of these key transcription factors in the cascade of gene expression involved in osteoblast differentiation. Runx2 has an osteoblast-specific isoform (Runx2-II) driven off the upstream promoter (20); this message was also suppressed 12-fold in Sh3 relative to Shlux ($p = 0.002$, data not shown) in a manner similar to the data for general Runx2 isoforms (Fig. 8*F*).

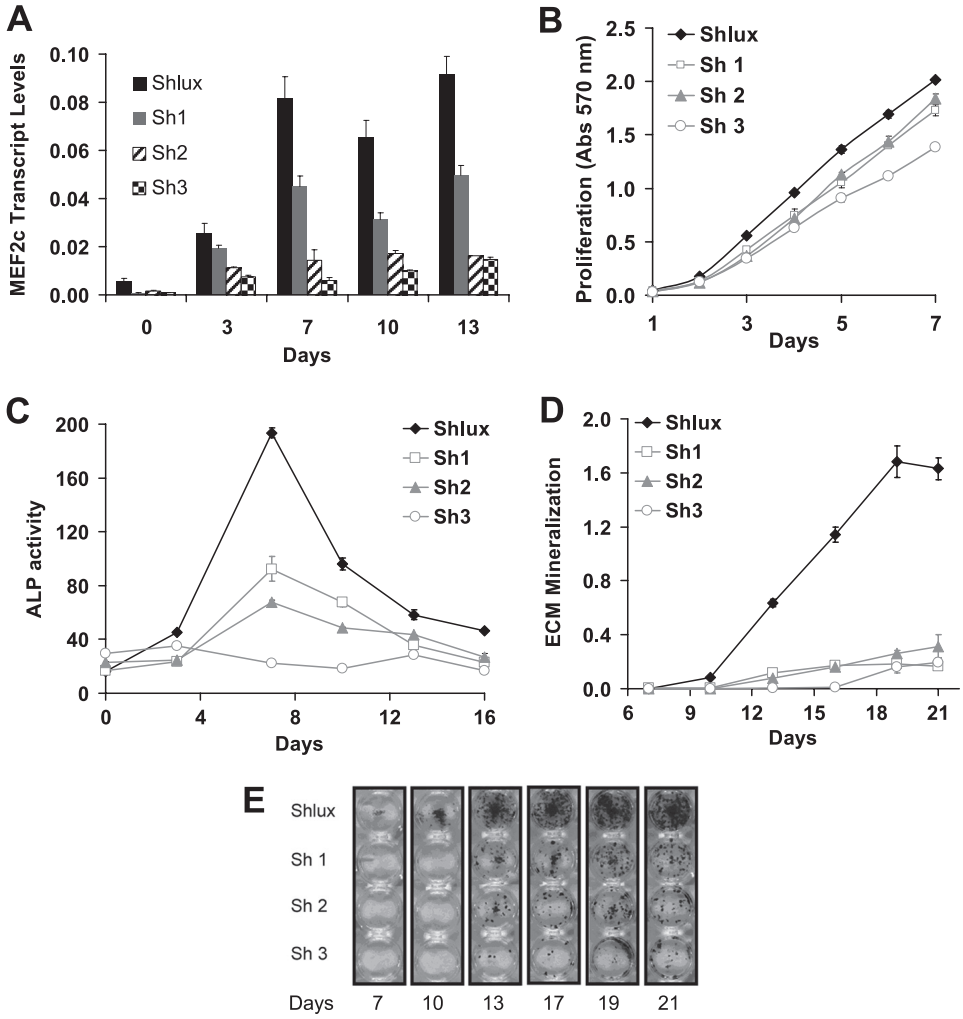


FIGURE 7. **shRNA-mediated silencing of *Mef2c* gene expression.** *A* shows the effectiveness of knockdown of *Mef2c* transcript levels in control (*Shlux, black columns*, a nontarget shRNA) compared with three cell lines, Sh1, Sh2, and Sh3 (*gray, striped,* and *checked columns,* respectively) with varying levels of *Mef2c* knockdown. Significant knockdown was obtained at all time points with the Sh3 cell line exhibiting the greatest extent of knockdown (*p* values not included because effects are large). Knockdown cell lines have a minor decrease in cell proliferation (*B*) that does not explain the extent of knockdown of ALP activity (*C*) or knockdown of mineralization, which is nearly total in all cell lines (*D*). Cell lines Sh1 and Sh2 that had very minor decrease in proliferation still had major suppression of mineralization. In addition, the appearance of visible bone nodules (Alizarin Red S stain, *E*) was delayed in *Mef2c* knockdown cell lines.

*Gene Expression in MC3T3-E1 Cells with Mef2c Knockdown*—To verify the finding that osteoblast differentiation was blocked by *Mef2c* knockdown, we investigated the consequences of *Mef2c* gene silencing on the expression of genes in cells undergoing osteoblast differentiation. Shlux and Sh3 cells were induced to differentiate into osteoblasts via the addition of OM and were harvested 3, 10, and 19 days for microarray gene expression analysis.

Low signal data (<100) were rejected, and genes were considered of interest if they were either highly induced, had high signal value that varied between day 3 and 10, or were different comparing control Shlux to the *Mef2c* knockdown cell line Sh3. The difference expected in *Mef2c* transcript level due to knockdown was observed in the array data (Fig. 9*A*). The top ranked genes for the absolute difference between day 3 and day 10 in control Shlux cells during growth in OM were mouse osteocalcin (*Bglap2*) and osteocalcin-related genes (*Bglap1* and *Bglap-rs1*). The next in rank were *Ibsp* and *Mmp13*. The osteocalcin-related genes (*Bglap1*, *Bglap2,* and *Bglap-rs1*), *Ibsp* and *Mmp13* were also the top rank of strongly suppressed genes in array comparison between Sh3 (*Mef2c* knockdown cell line, Fig. 9, *B–D*) and Shlux, confirming that the array detected the same gene changes as seen previously using qPCR. These observations validated the array as a discovery tool to identify candidates for further work related to *Mef2c* action in osteoblasts. Regulated genes that are highly expressed on the array and that were represented by multiple probes sets in the array platform are presented in Fig. 9. The parathyroid hormone receptor (*Pthr1*) was identified as increased by DMSO (Table 2); *Pthr1* was significantly increased during osteoblast differentiation in Shlux and was suppressed in the Sh3 cell line (Fig. 9*E*) suggesting positive regulation of *Pthr1* by Mef2c. Collagen type 2 $\alpha$1 (*Col2a1*) was similarly affected by *Mef2c* knockdown (Fig. 9*F*). As expected, both *Runx2* and osterix transcripts were significantly reduced on the array (Fig. 9, *G* and *H*), consistent with the analysis using qPCR (see Fig. 8). Numerous other genes were affected by *Mef2c* knockdown, consistent with a global effect of Mef2c on gene expression in MC3T3-E1 cells. The data suggest that Mef2c transcription factor is required for appropriate expression of the suite of osteoblast-specific genes that

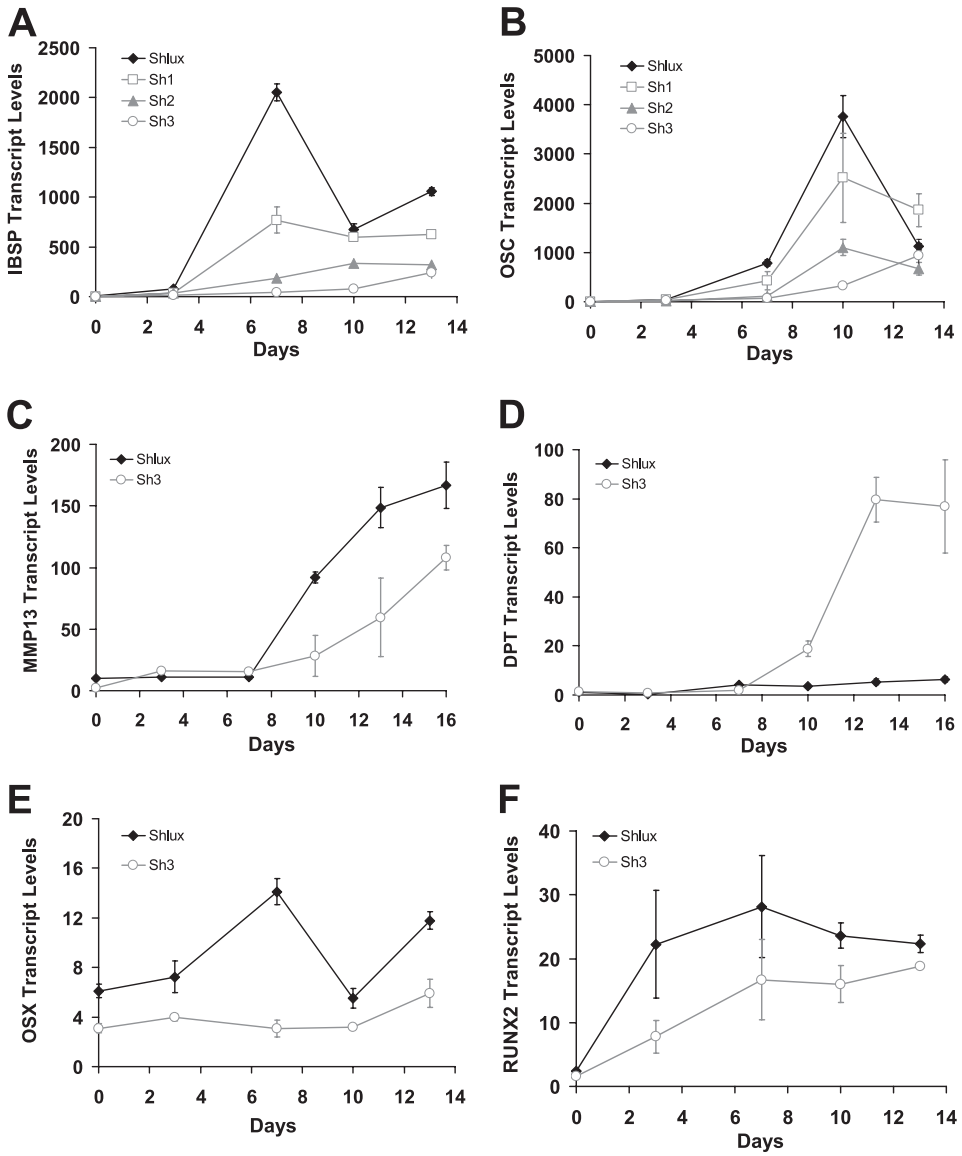


FIGURE 8. **Mef2c knockdown results in flow on knockdown of osteoblast-specific genes.** qPCR was used to determine transcript levels for candidate osteoblast-related genes. Those genes that were induced by DMSO were repressed by Mef2c knockdown. Integrin-binding sialoprotein (*IBSP*, *A*) and osteocalcin (*OCS*, *B*) were knocked down in a manner correlated with the extent of *Mef2c* knockdown in Sh1, Sh2, and Sh3, compared with control Shlux. The most extreme knockdown line Sh3 was then examined. Matrix metalloproteinase 13 (*MMP13*, *C*) showed flow on knockdown (*C*), and dermatopontin (*DPT*, *D*) shows the reverse effect; flow on gene induction resulted from *Mef2c* knockdown, suggesting that Mef2c acts as a repressor of this gene. Comparing Mef2c knockdown cell line Sh3 with control (*Shlux*) demonstrated similar flow on knockdown of osteoblast transcription factors osterix ($p = 0.001$, *E*) and *Runx2* ($p = 0.004$, *RUNX2, F*). Transcript levels are relative to zero time in OM, except for osterix that was different at zero time, *i.e.* transcript levels of osterix were already detectably different prior to culture in OM. *p* values in experiments *A–D* are all $<10^{-6}$ for the overall effect in the generalized linear model.

characterizes the cell phenotype and ultimately results in mineralizing activity. Tables 3 and 4 contain the genes displaying the largest fold changes in expression, regardless of magnitude of expression, between the two cell lines at each of the time points.

Finally, the osteocyte marker gene sclerostin (*Sost*) was also evaluated as the *Sost* promoter is a proposed target gene of Mef2c in osteocytes (21). In our hands, *Sost* expression was not detected in differentiating MC3T3-E1 cells, either with DMSO or not, or with *Mef2c* knockdown, in any experiment using qPCR, indicated by nondetected cycle threshold values (data not shown). No array probe set showed signal over background in any array experiment. The absence of sclerostin expression suggests that under any of the conditions reported in this study, MC3T3-E1 cells do not acquire an osteocyte phenotype.

## DISCUSSION

In this study, we showed that DMSO treatment was able to stimulate mineralization of human osteoblasts in primary culture. Increasing the mineralization potential of such cells may be useful in tissue engineering for replacement of mineralized tissues. Similarly, primary adipose-derived mesenchymal cells were stimulated by DMSO to produce more mineral, as were primary mouse calvarial cells, suggesting that DMSO enhancement is a general phenomenon applicable to osteoblast culture.

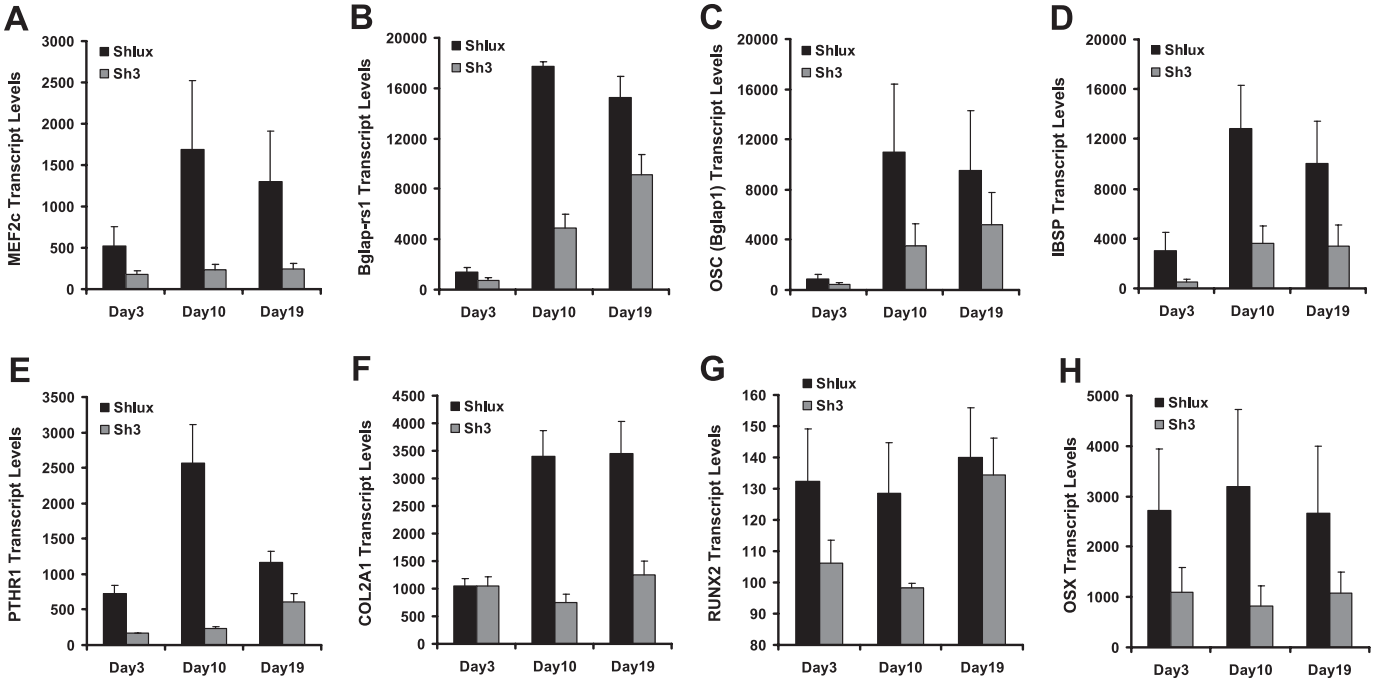


FIGURE 9. **Differential expression of osteoblast-related genes resulting from *Mef2c* knockdown.** Shlux and Sh3 cells were induced to differentiate into osteoblasts via the addition of OM. Cells were harvested 3, 10, and 19 days in OM for whole genome microarray gene expression analysis. Genes with large changes in absolute signal and with repeated probe sets on array are shown. Significant differences were observed for *Mef2c* (*A*, *MEF2C*), osteocalcin-related sequences (*Bglap-rs1*, *B*), osteocalcin (*OSC*, *C*), integrin-binding sialoprotein (*IBSP*, *D*), parathyroid hormone receptor (*PTHR1*, *E*), $\alpha$1 chain of type 2 collagen (*COL2A1*, *F*), transcription factors *Runx2* (*RUNX2*, *G*), and osterix (*OSX*, *H*). Transcript levels represent the microarray intensity values, and *error bars* are S.E.; significance was based on two-factor analysis of variance using all time points and all data values ($p$ values are all $<0.006$ for effect of *Mef2c* knockdown, except *Runx2,* which has $p = 0.03$).

**TABLE 3**

**Genes with higher expression in *Mef2c* shRNA knockdown cells (Sh3)**

Genes that exhibit higher expression after Mef2c knockdown (Sh3) relative to control (Shlux) at days 3, 10, and 19 during osteoblast differentiation. For these genes, knockdown of Mef2c results in increased expression in Sh3 cells. Fold represents the ratio of gene expression, Sh3 relative to Shlux.

| Day 3 | | | Day 10 | | | Day 19 | | |
|---|---|---|---|---|---|---|---|---|
| Symbol | Accession | Fold | Symbol | Accession no. | Fold | Symbol | Accession no. | Fold |
| *Ly6a* | NM_010738 | 3.9 | *Ccl7* | NM_013654 | 7.5 | *Ccl7* | NM_013654 | 7.1 |
| *Tnnc1* | NM_009393 | 3.2 | *Abi3bp* | NM_178790 | 4.6 | *Abi3bp* | NM_178790 | 5.9 |
| *Ly6c1* | NM_010741 | 3.2 | *Ly6a* | NM_010738 | 4.6 | *Ly6a* | NM_010738 | 5.1 |
| *Loc100047583* | XM_001479138 | 2.76 | Scl0002547.1_9 | scl0002547.1_9 | 4.1 | *Nme7* | NM_138314 | 4.8 |
| *Tgm2* | NM_009373 | 2.7 | *Ifi27* | NM_029803 | 4.0 | *Txnip* | NM_023719 | 4.4 |
| *Gdpd2* | NM_023608 | 2.5 | *Txnip* | NM_023719 | 3.8 | *Ecrg4* | NM_024283 | 4.4 |
| *Pappa* | NM_021362 | 2.4 | *Ccl5* | NM_013653 | 3.7 | *Htra3* | NM_030127 | 4.2 |
| *6330406i15rik* | NM_027519 | 2.4 | *Dcn* | NM_007833 | 3.5 | *Atp1b1* | NM_009721 | 3.8 |
| *Wisp2* | NM_016873 | 2.3 | *Klra4* | NM_010649 | 3.5 | *Mfap4* | NM_029568 | 3.7 |
| *Nme7* | NM_138314 | 2.3 | *Ly6c1* | NM_010741 | 3.5 | *Papss1* | NM_011863 | 3.6 |
| *Loc382972* | XM_356781 | 2.3 | *1500015o10rik* | NM_024283 | 3.2 | *Robo1* | NM_019413 | 3.4 |
| *Idb4* | AK041164 | 2.2 | *Figf* | NM_010216 | 3.0 | *Ly6c1* | NM_010741 | 3.3 |
| *Ifit3* | NM_010501 | 2.2 | *Loc100038894* | XM_001471776 | 3.0 | *Chst2* | NM_018763 | 3.1 |
| *6330406i15rik* | NM_027519 | 2.2 | *Ccl2* | NM_011333 | 3.0 | *Htra1* | NM_019564 | 3.1 |
| *Ppap2b* | NM_080555 | 2.1 | *Tnn* | NM_177839 | 2.9 | *Mrgprf* | NM_145379 | 3.1 |
| *B230343a10rik* | scl41403.1.1_37 | 2.1 | *Lum* | NM_008524 | 2.9 | *Casp1* | NM_009807 | 3.0 |
| *Abca3* | NM_013855 | 2.1 | *Syt1* | NM_009306 | 2.9 | *Alox5ap* | NM_009663 | 3.0 |
| *Nme7* | NM_138314 | 2.1 | *Txnip* | NM_001009935 | 2.9 | *Il33* | NM_133775 | 3.0 |
| *Cdkl5* | NM_001024624 | 2.1 | *Cdkl5* | NM_001024624 | 2.9 | *Cxx1a* | NM_024170 | 3.0 |
| *Sdpr* | NM_138741 | 2.1 | *Id4* | NM_031166 | 2.8 | *Pigt* | NM_133779 | 2.9 |

We then used the pre-osteoblast cell line MC3T3-E1 to investigate DMSO-enhanced osteoblast differentiation and as a tool to identify novel regulators of differentiation. We first established the optimal DMSO concentration required to enhance differentiation through dose-response curves. We next investigated the impacts of DMSO-enhanced differentiation through time course experiments. The results showed that DMSO facilitated increases in ALP activity and mineralization, and the increases were sustained throughout differentiation. It seems likely that DMSO-treated cells achieved a heightened state of differentiation reflected by an enhanced capacity to mineralize the surrounding extracellular matrix. Cheung *et al.* (12) examined *Runx2* and osterix induction by DMSO in normal $\alpha$-MEM at 5 days only; *Runx2* (1.89-fold) and osterix (1.39-fold) induction by DMSO was significant. In contrast, we examined the effect of DMSO on target gene expression using a number of target genes at numerous time points in OM; in particular, we observed strong induction of osterix by DMSO over the entire

**TABLE 4**

**Genes displaying increased expression in control cells (Shlux) compared with *Mef2c* shRNA knockdown (Sh3) cells at days 3, 10, and 19 during osteoblast differentiation**

Fold indicates change in Shlux relative to Sh3. Analysis is based on fold change.

| Day 3 | | | Day 10 | | | Day 19 | | |
|---|---|---|---|---|---|---|---|---|
| Symbol | Accession | Fold | Symbol | Accession | Fold | Symbol | Accession | Fold |
| *Panx3* | NM_172454 | 10.6 | *Cdsn* | NM_001008424 | 11.4 | *Spata19* | NM_029299 | 14.2 |
| *Ibsp* | NM_008318 | 7.1 | *Trib3* | NM_175093 | 10.3 | *Timp4* | NM_080639 | 13.8 |
| *Mest* | NM_008590 | 4.5 | *Megf10* | NM_00100197 | 9.9 | *Col10a1* | NM_009925 | 10.4 |
| *Smpd3* | NM_021491 | 4.4 | *Cox6a2* | NM_009943 | 8.3 | *Panx3* | NM_172454 | 7.7 |
| *Pthr1* | NM_011199 | 4.3 | *Pthr1* | NM_011199 | 8.0 | *Cox6a2* | NM_009943 | 7.7 |
| *Ifitm5* | NM_053088 | 4.2 | *Chac1* | NM_026929 | 6.5 | *Trib3* | NM_175093 | 7.4 |
| *H19* | NR_001592 | 3.6 | *Sema7a* | NM_011352 | 6.3 | *Megf10* | NM_001001979 | 7.3 |
| *Tnfrsf19* | NM_013869 | 3.5 | *Aldh1l2* | NM_153543 | 6.2 | *Mef2c* | NM_025282 | 6.7 |
| *Ramp1* | NM_016894 | 3.4 | *Mef2c* | NM_025282 | 6.1 | *Krt14* | NM_016958 | 6.4 |
| *Mef2c* | NM_025282 | 3.3 | *Panx3* | NM_172454 | 6.0 | *Cdsn* | NM_001008424 | 5.5 |
| *Tmem176b* | NM_023056 | 3.2 | *Ptgis* | NM_008968 | 5.7 | *Ptgis* | NM_008968 | 5.1 |
| *Tnnc2* | NM_009394 | 2.8 | *Col10a1* | NM_009925 | 5.5 | *Fam180a* | NM_173375 | 4.6 |
| *Nupr1* | NM_019738 | 2.6 | *Nupr1* | NM_019738 | 5.0 | *Fam20a* | NM_153782 | 4.2 |
| *Timp4* | NM_080639 | 2.5 | *Scx* | NM_198885 | 5.0 | *Aldh1l2* | NM_153543 | 4.1 |
| *Akp2* | NM_007431 | 2.5 | *Ramp1* | NM_016894 | 4.8 | *Loxl4* | NM_053083 | 4.0 |
| *C1qtnf3* | NM_030888 | 2.4 | *Fam180a* | NM_173375 | 4.7 | *Ibsp* | NM_008318 | 4.0 |
| *Tnc* | NM_011607 | 2.3 | *Slc6a9* | NM_008135 | 4.5 | *Gper* | NM_029771 | 4.0 |
| *Sp7* | NM_130458 | 2.3 | *Ddit3* | NM_007837 | 4.4 | *Slc40a1* | NM_016917 | 4.0 |
| *Srpx2* | NM_026838 | 2.2 | *Fabp3* | NM_010174 | 4.3 | *Chac1* | NM_026929 | 3.6 |
| *Wif1* | NM_011915 | 2.2 | *Fam20a* | NM_153782 | 4.2 | *Unc5b* | NM_029770.2 | 3.6 |

time period of mineralization, including days 3 and 5. In addition, we defined *Mef2c* as a target of DMSO induction. A critical period of the first 3 days was seen where DMSO exposure was sufficient to generate the maximal enhancement, a fact that may prove useful in tissue engineering. Investigations of that 3-day period showed that endogenous osterix was significantly elevated at 3 days of treatment with DMSO and that enhancement of a transfected osteocalcin promoter can occur within that period. Although the mechanism of the DMSO effect remains to be elucidated, it seems likely that the mechanism will involve transcription factors. Further work is needed to fully define the early effects of DMSO on gene expression in osteoblasts. DMSO has other effects in bone biology. Zyuz'kov *et al.* (31) show that DMSO treatment (for 5 days at 2 g/kg) via a gastric tube in mice results in a decrease of colony-forming units-fibroblast (CFU-F) derived from the stromal fraction in bone marrow cultures at 8 days. We also tested DMSO on osteoclast differentiation and found profound stimulation, particularly in the size of osteoclasts.[3] To our knowledge, no experiments have been reported specifically addressing bone anabolic effects of DMSO *in vivo*. A more complete analysis of the effects of DMSO on bone *in vivo* is warranted, as osteoblasts, osteoclasts, and stromal cells may be affected by DMSO.

Gene expression studies revealed that osterix, *Ibsp*, osteocalcin, and *Mmp13* were increased as a consequence of DMSO treatment and provided evidence that key regulators of osteoblast function were altered by DMSO, consistent with an enhanced state of osteoblast differentiation. Microarray analysis revealed Mef2c as a novel factor involved in osteoblast differentiation. Mef2c is a MADS-box transcription factor that has pleiotropic effects with examples including heart development (22), cardiac hypertrophy (23), myeloid cell fate (24), and skeletal muscle differentiation (25), among many other effects. In addition, the *Mef2c* locus has recently been linked genetically to human bone mineral density (26). More germane to bone mineralization are the observations of Arnold *et al.* (27), using various conditional *Mef2c* knock-out mice, that *Mef2c* is expressed in hypertrophic chondrocytes and is involved in endochondral ossification. Our *ex vivo* models suggest that *Mef2c* is not restricted to the chondrocyte but functions as a key osteoblast transcription factor upstream of both Runx2 and osterix in osteoblasts. We detected reasonable expression of *Col2a1*, at least in MC3T3-E1 cells by gene array. Sakaia *et al.* (28) detected expression of the *Col2a1* promoter in mouse osteoblasts *in vivo*, using a $\beta$-galactosidase indicator line (Rosa26) crossed with a *Col2A1* promoter driving CRE, suggesting some commonality between chondrocytes and osteoblasts. Arnold *et al.* (27) reported that the *Col2A1* promoter was regulated by Mef2c. Consistent with that fact, we observed flow on knockdown of *Col2A1* in *Mef2c* knockdown cell lines. Combining these lines of evidence, it seems likely that Mef2c acts in osteoblasts as well as chondrocytes.

Transcript profiling revealed *Mef2c* was dynamically regulated during MC3T3-E1 osteoblast differentiation and increased during primary calvarial osteoblast differentiation. In MC3T3-E1 cells, two distinct peaks in *Mef2c* gene expression were observed and coincided with the developmentally relevant time points (29) on day 7, where the cells slow their proliferation and begin to differentiate, and on days 16–19, where cells enter the terminal stages of differentiation and actively mineralize. The addition of DMSO to the culture medium resulted in an accelerated pattern of *Mef2c* gene expression whereby the first peak in expression was earlier and the second peak more substantial. Notably, the expression of *Mef2c* during the terminal stages of differentiation (days 13–19) was significantly elevated in DMSO-treated cells introducing the possibility that Mef2c could function as a regulator of mineralization.

Immunohistochemical analysis showed Mef2c in embryonic and adult mouse in cells associated with bone. Although

[3] N. A. Morrison and S. R. Stephens, unpublished data.

such cells were not formally identified as osteoblasts using other markers, it seems reasonable to conclude that osteoblasts express Mef2c. Furthermore, transfection of *Mef2c* expression vector into MC3T3-E1 cells resulted in increased osteocalcin transcript and increased alkaline phosphatase activity suggesting that Mef2c can function in osteoblasts. Short hairpin-mediated gene knockdown in MC3T3-E1 cells confirmed the functional role for Mef2c in osteoblast differentiation. The consistent knockdown of *Mef2c* mRNA levels was linked to potent reductions in ALP activity throughout differentiation. ALP participates in inorganic phosphate homeostasis and is associated with matrix vesicle mineralization (30). Therefore, it was not surprising to observe that mineralization was also disrupted in *Mef2c* shRNAi-expressing cells. Furthermore, the key osteoblast-specific gene, osteocalcin, was suppressed in *Mef2c* knockdown cell lines, and of all genes assayed by gene array, the osteocalcin-related gene clusters (*Bglap1, Bglap2,* and *Bglap-rs1*) were the top rank of genes altered by *Mef2c* knockdown. The data suggest an essential role for Mef2c in regulating osteoblast differentiation.

A potential mechanism by which Mef2c could regulate osteoblast differentiation is controlling the expression of Runx2 and osterix, which were both significantly knocked down at the mRNA level as a flow on from *Mef2c* knockdown. This possibility is strengthened by the fact that osteocalcin is known to be regulated directly by Runx2 and osterix. Further work is needed to determine whether Mef2c has a direct or indirect effect on the osteocalcin promoter. The comparative analysis of gene expression between Shlux and Sh3 cells using microarrays revealed many differentially regulated genes, consistent with Mef2c being necessary for the maintenance of osteoblast-specific gene expression. Notably, the lowered expression of several known osteoblast regulators (such as *Akp2, Ibsp, Mmp13,* and *Pthr1*) indicated Sh3 cells had a general inability to differentiate correctly.

We could not detect *Sost* expression using qPCR or gene array, arguing strongly that the DMSO-treated cells do not adopt an osteocyte-like phenotype. Mef2c is proposed to mediate the regulation of the Sost enhancer by parathyroid hormone (21). In our study, *Mef2c* knockdown resulted in flow on knockdown of *Pthr1* (the parathyroid hormone receptor), suggesting an alternative connection between Mef2c and parathyroid hormone that may operate in osteoblasts. This can be clarified in future studies.

In conclusion, we have demonstrated that DMSO has profound effects on the differentiation of human osteoblasts, mouse adipocyte-derived primary cells, mouse calvarial osteoblasts, and the model cell line MC3T3-E1. Treatment with DMSO resulted in highly significant increases in ALP activity and mineral deposition in each of these osteoblastic cell models. We used DMSO-enhanced MC3T3-E1 differentiation as a tool to screen for factors involved in the developmental process. Our search identified Mef2c as a candidate osteoblast transcription factor, whose expression was verified in mouse primary calvarial cells. shRNAi-mediated gene silencing in MC3T3-E1 cells demonstrated that *Mef2c* was required for proper osteoblast differentiation and function. Our data suggest Mef2c has an important role in osteoblast biology and is required for proper osteoblast differentiation and matrix mineralization. We suggest that Mef2c is a key osteoblast transcription factor, upstream of Runx2 and osterix, and is worthy of further study in osteoblast biology. Combined with its role in chondrocyte hypertrophy, osteoblast biology (this study), and its presence in osteocytes, Mef2c is positive regulator of skeletal formation, mineralization, and homeostasis at a number of levels.

## REFERENCES


1. Karsenty, G. (2003) *Nature* **423,** 316–318
2. Hadjidakis, D. J., and Androulakis, I. I. (2006) *Ann. N.Y. Acad. Sci.* **1092,** 385–396
3. Franceschi, R. T. (1999) *Crit. Rev. Oral. Biol. Med.* **10,** 40–57
4. Weiss, A. J., Iqbal, J., Zaidi, N., and Mechanick, J. I. (2010) *Curr. Osteoporos. Rep.* **8,** 168–177
5. Aubin, J. E., Liu, F., Malaval, L., and Gupta, A. K. (1995) *Bone* **17,** 77S–83S
6. Marie, P. J. (2008) *Arch. Biochem. Biophys.* **473,** 98–105
7. Komori, T. (2006) *J. Cell. Biochem.* **99,** 1233–1239
8. Hassan, M. Q., Tare, R., Lee, S. H., Mandeville, M., Weiner, B., Montecino, M., van Wijnen, A. J., Stein, J. L., Stein, G. S., and Lian, J. B. (2007) *Mol. Cell. Biol.* **27,** 3337–3352
9. Wu, M., Hesse, E., Morvan, F., Zhang, J. P., Correa, D., Rowe, G. C., Kiviranta, R., Neff, L., Philbrick, W. M., Horne, W. C., and Baron, R. (2009) *Bone* **44,** 528–536
10. Santos, N. C., Figueira-Coelho, J., Martins-Silva, J., and Saldanha, C. (2003) *Biochem. Pharmacol.* **65,** 1035–1041
11. Woods, E. J., Perry, B. C., Hockema, J. J., Larson, L., Zhou, D., and Goebel, W. S. (2009) *Cryobiology* **59,** 150–157
12. Cheung, W. M., Ng, W. W., and Kung, A. W. (2006) *FEBS Lett.* **580,** 121–126
13. Potthoff, M. J., and Olson, E. N. (2007) *Development* **134,** 4131–4140
14. Gregory, C. A., Gunn, W. G., Peister, A., and Prockop, D. J. (2004) *Anal. Biochem.* **329,** 77–84
15. Chomczynski, P., and Sacchi, N. (1987) *Anal. Biochem.* **162,** 156–159
16. Vandesompele, J., De Preter, K., Pattyn, F., Poppe, B., Van Roy, N., De Paepe, A., and Speleman, F. (2002) *Genome Biol.* **3,** RESEARCH0034
17. Zang, M. X., Li, Y., Wang, H., Wang, J. B., and Jia, H. T. (2004) *J. Biol. Chem.* **279,** 54258–54263
18. Lassaux, A., Sitbon, M., and Battini, J. L. (2005) *J. Virol.* **79,** 6560–6564
19. Ortuño, M. J., Ruiz-Gaspà, S., Rodríguez-Carballo, E., Susperregui, A. R., Bartrons, R., Rosa, J. L., and Ventura, F. (2010) *J. Biol. Chem.* **285,** 31985–31994
20. Xiao, Z., Awad, H. A., Liu, S., Mahlios, J., Zhang, S., Guilak, F., Mayo, M. S., and Quarles, L. D. (2005) *Dev. Biol.* **283,** 345–356
21. Leupin, O., Kramer, I., Collette, N. M., Loots, G. G., Natt, F., Kneissel, M., and Keller, H. (2007) *J. Bone Miner. Res.* **22,** 1957–1967
22. Bi, W., Drake, C. J., and Schwarz, J. J. (1999) *Dev. Biol.* **211,** 255–267
23. Xu, J., Gong, N. L., Bodi, I., Aronow, B. J., Backx, P. H., and Molkentin, J. D. (2006) *J. Biol. Chem.* **281,** 9152–9162
24. Schüler, A., Schwieger, M., Engelmann, A., Weber, K., Horn, S., Müller, U., Arnold, M. A., Olson, E. N., and Stocking, C. (2008) *Blood* **111,** 4532–4541
25. Potthoff, M. J., Arnold, M. A., McAnally, J., Richardson, J. A., Bassel-Duby, R., and Olson, E. N. (2007) *Mol. Cell. Biol.* **27,** 8143–8151
26. Rivadeneira, F., Styrkársdottir, U., Estrada, K., Halldórsson, B. V., Hsu, Y. H., Richards, J. B., Zillikens, M. C., Kavvoura, F. K., Amin, N., Aulchenko, Y. S., Cupples, L. A., Deloukas, P., Demissie, S., Grundberg, E., Hofman, A., Kong, A., Karasik, D., van Meurs, J. B., Oostra, B., Pastinen, T., Pols, H. A., Sigurdsson, G., Soranzo, N., Thorleifsson, G., Thorsteinsdottir, U., Williams, F. M., Wilson, S. G., Zhou, Y., Ralston, S. H., van Duijn, C. M., Spector, T., Kiel, D. P., Stefansson, K., Ioannidis, J. P., and Uitterlinden, A. G. (2009) *Nat. Genet.* **41,** 1199–1206
27. Arnold, M. A., Kim, Y., Czubryt, M. P., Phan, D., McAnally, J., Qi, X.,

Shelton, J. M., Richardson, J. A., Bassel-Duby, R., and Olson, E. N. (2007) *Dev. Cell.* **12,** 377–389
28. Sakai, K., Hiripi, L., Glumoff, V., Brandau, O., Eerola, R., Vuorio, E., Bösze, Z., Fässler, R., and Aszódi, A. (2001) *Matrix Biol.* **19,** 761–767
29. Quarles, L. D., Yohay, D. A., Lever, L. W., Caton, R., and Wenstrup, R. J. (1992) *J. Bone Miner. Res.* **7,** 683–692
30. Balcerzak, M., Hamade, E., Zhang, L., Pikula, S., Azzar, G., Radisson, J., Bandorowicz-Pikula, J., and Buchet, R. (2003) *Acta Biochim. Pol.* **50,** 1019–1038
31. Zyuz'kov, G. N., Gur'yantseva, L. A., Simanina, E. V., Zhdanov, V. V., Dygai, A. M., and Goldberg, E. D. (2007) *Bull. Exp. Biol. Med.* **143,** 535–538